Investigations of the role of neoclassical transport in ion-root plasmas on W7-X

N. Pablant[1], A. Langenberg[2], A. Alonso[4], J. Baldzuhn[2], C.D. Beidler[2], L.G. Bötteger[9,2], S. Bozhenkov[2], R. Burhenn[2], K.J. Brunner[2], A. Dinklage[2], G. Fuchert[2], O. Ford[2], D.A. Gates[1], J. Geiger[2], O. Grulke[9,2], M. Hirsch[2], U. Höfel[2], Z. Huang[10], Y. Kazakov[8], J. Knauer[2], M. Krychowiak[2], J. Kring[5], H. Laqua[2], M. Landreman[7], S. Lazerson[1], H. Maaßberg[2], O. Marchuck[3], A. Mollen[2], E. Pasch[2], A. Pavone[2], M. Porkolab[10], S. Satake[6], T. Schröder[2], H. Smith[2], J. Svensson[2], P. Traverso[5], Y. Turkin[2], J.L. Velasco[4], A. Von Stechow[2], F. Warmer[2], G. Weir[2], R.C. Wolf[2], D. Zhang2[2] and the W7-X Team

[1]Princeton Plasma Physics Laboratory, USA
[2]Max-Planck-Institut für Plasmaphysik, Germany
[3]Forschungszentrum Jülich, Germany
[4]Laboratorio Nacional de Fusión, CIEMAT, Spain
[5]Auburn University, USA
[6]National Institute for Fusion Science, Japan
[7]University of Maryland, USA
[8]Chalmers University of Technology, Göteborg, Sweden
[9]Technical University of Denmark, Denmark
[10]Massachusetts Institute of Technology, USA
[11]SUNY Cortland, USA

Corresponding Author: npablant@pppl.gov

Abstract:

The role of the radial electric field in high performance ion-root plasmas on Wendelstein 7-X (W7-X) is examined and compared with neoclassical predictions. The W7-X stellarator is the world's first large scale optimized stellarator. One of the important targets chosen for optimization during the W7-X design process was the reduction of core neoclassical heat transport. This optimization was targeted for reactor relevant high-density plasmas with $T_e \approx T_i$ in which the neoclassical ambipolar radial electric field is expected to negative throughout the plasmas core.

Measurements of the core radial electric field (E_r) have confirmed that ion-root conditions (negative E_r in the plasma core) have been achieved in W7-X with high-density plasmas and central ERCH. These measured Er profiles agree well with the neoclassical ambipolar Er predicted by the code SFINCS. This good agreement provides confidence in the validity of neoclassical calculations in high-density ion-root conditions, and enables initial studies on the role of neoclassical transport in the optimized high-density regime of W7-X.

Profile measurements of electron temperature (T_e), ion temperature (T_i) and electron density (ne) along with approximations for the average value of Zeff have been used as inputs to the SFINCS code to calculate the ambipolar E_r profile along with neoclassical ion and electron heat flux profiles (Q_{NCi}, Q_{NCe}). Finally the total experimental energy input to the plasma from ECRH heating has been compared to the neoclassical heat fluxes to provide a first estimate for the fraction of transport that can be attributed to neoclassical processes in reactor relevant high-density ion-root conditions.

1 Introduction

The W7-X stellarator is the world's first large scale optimized stellarator[1, 2]. One of the important targets chosen for optimization during the W7-X design process was the reduction of core neoclassical heat transport[3]. This optimization was targeted for reactor relevant[4] high-density ECRH heated plasmas with $T_e \approx T_i$ in which the neoclassical ambipolar radial electric field is expected to negative throughout the plasmas core. Before the effectiveness of the optimization can be studied, it is important to first achieve these high-density conditions and experimentally validate the use of our current neoclassical codes.

In stellarator plasmas the neoclassical particle fluxes are not intrinsically ambipolar; this leads to the generation of a radial electric field profile (E_r) that provides for ambipolarity across the plasma radius. Furthermore, in the absence of significant fast ion losses, the radial electric field is thought to be fully described by neoclassical theory as turbulent particle transport is expected to be intrinsically ambipolar. The details of the Er profile are expected to have a strong effect on the heat, particle, and impurity fluxes as well as the bootstrap current [5, 6].

2 Diagnostic Method

Experimental radial electric field profiles are inferred from measurements of the perpendicular velocity ($u_\perp$)[7], as provided by the x-ray imaging crystal spectrometer (XICS) diagnostic. To derive the radial electric field from the flux surface averaged perpendicular flow velocity ($U_\perp$) the radial force balance equation can be used: $\langle E_r \rangle = (1/en_I Z_I)\partial p_I/\partial\rho\langle|\nabla\rho|\rangle - \langle u_\perp B\rangle$, where p_I, n_I and Z_I denote the pressure, density and charge of the ion species being measured. The pressure gradient term is small for Ar^{16+} where this term is weighted by $1/Z_I = 1/16$ and has been neglected in the current calculations.

The XICS diagnostic is based on spectroscopic analysis of emission from highly charged argon impurities that are seeded into the plasma in trace amounts[8]. The XICS system records a 1D image of line integrated spectra. These line integrated signals can be used to find local plasma parameters by utilizing tomographic inversion techniques with a known equilibrium [9, 10]. Standard Doppler spectroscopy techniques are used to extract information from the recorded spectra: Ion temperatures (T_i) are found from the line widths, electron temperatures (T_e) from line ratios, plasma flow (u) from the line shifts, and impurity densities ($n_{Ar^{15+/16+/17+}}$) from the line amplitudes[8]. The viewing geometry of the XICS system, which is close to lying in a poloidal plane, causes the flow measurements to be primarily sensitive to the component of the velocity that is perpendicular to the magnetic field ($u_\perp$) (see Ref. 7 Fig. 1).

Detailed descriptions of the XICS diagnostic can be found in Ref. 11 and Ref. 12 and the diagnostic concept has been explained in detail by Bitter *et al.* in Ref. 8.

The procedure for determining the E_r profile from the line-integrated XICS measurements is essentially the same as described in Ref. 7 , but with the following improvements: First, in the inversion of the emissivity (which is the first step in the inversion process) a simple parameterization that allows the emissivity to vary poloidally on a flux surface has now been added. It has been found that in many W7-X plasmas, particularly before boronization, that the measured Ar^{16+} emissivity was not completely consistent with the assumption of constant density/emissivity on a flux surface. The source of this asymmetry is not yet known, however a possible explanation is that it is due to Ar charge exchange with neutral hydrogen. Second, an emperical correction for the zero wavelength location on the detector has been added on top of the standard geometry/wavelength calibration. This correction has been implemented as a quadratic offset from the nominal zero wavelength across the detector, and is determined by using a reference plasma where a long period of time averaging can be used to provide improved signal to noise for the calibration. The need for this emperical correction is likely due to subtle errors in the characterization of the hardware dimensions.

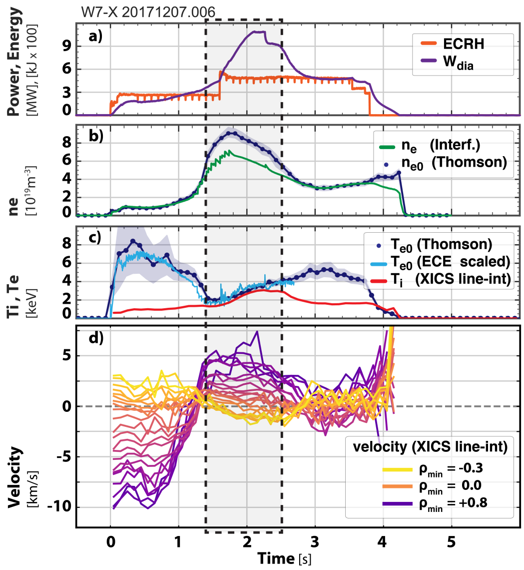

FIG. 1: Time traces for program 20171207.006. Cryogenic hydrogen pellets are injected from 1.2 s *to* 1.8 s. *The time when the radial electric field is fully within the ion-root is highlighted with the dashed box. Electron temperature and density taken from the central Thomson channels. Fig. (d): Line-integrated plasma for several XICS sightlines; purple and yellow lines represent views above and below the magnetic axis respectively. The change in the direction of the plasma direction can be clearly seen in these non-inverted measurements.*

3 Observation of ion-root in pellet fueled plasmas

For the current analysis a plasma program is chosen that includes cryogenic hydrogen pellet injection[13] and central ECRH heating, see Fig.1. During the Op1.2 experimental campaign the available pellet injection system was limited to an operational time of 1 s. This limitation results in a highly transient high density phase in the plasma evolution. While the plasmas conditions are non-stationary, the neoclassical radial electric field is expected to change on the same timescale as the temperature and density evolution and can still be analyzed. It should be noted that the program that will be the focus of the subsequent analysis is not unique, and that many plasmas with similar time-histories have

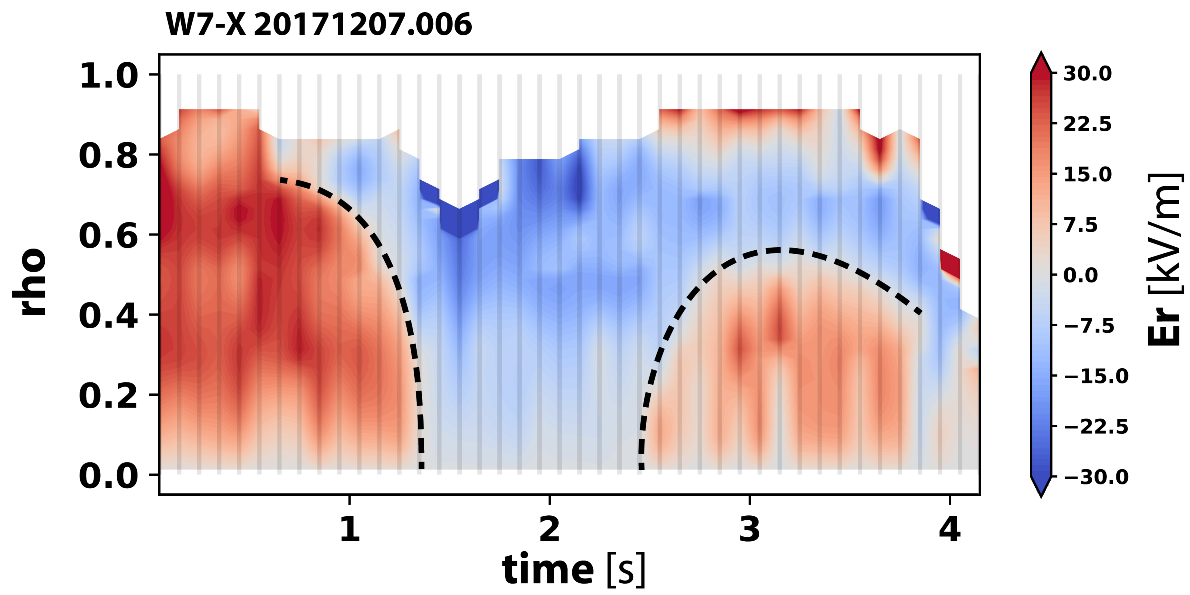

FIG. 2: Inverted radial electric field as inferred from XICS measurements. Raw data has been binned prior to inversion to provide 100 ms *time resolution and* 3 cm *spatial resolution. Vertical lines denote actual measurement times (center of integration window); color between lines is interpolated. In the time around after* 1.5 s *a strong peaking in the* Ar^{16+} *emissivity profile results in a limited measurable profile extent; radii with insufficient signal for valid measurements are left white. The dashed lines indicates the* E_r *inversion radius which the radial electric field changes sign.*

been produced at W7-X.

Program 20171207.006 starts with a low density plasma with 2.0 MW of central ECRH heating. From 1.2 s to 1.8 s hydrogen pellets are injected into the plasma with a frequency of 30 Hz. After the start of the pellet injection additional central ECRH heating power is added to bring the total injected power to 5.0 MW. During pellet injection the electron density rises to a value of $0.9 \times 10^{20}\,\mathrm{m}^{-3}$ and also becomes peaked, as can be seen by the separation of the central density from the line-integrated density in Fig.1b. Immediately after pellet injection the electron temperature falls to meet the ion temperature; after reaching equilibration both the T_e and T_i profiles begin to increase together, ultimately reaching an equilibrated core temperature of 3.7 keV at 2.1 s. During this period of collisionality coupled heating the stored energy increases dramatically up to a value of 1.2 MJ.

The evolution of the radial electric field profiles from this program, which are inferred from the XICS diagnostic, are shown in Fig.2.These measurements confirm the expected existence of a negative radial electric field in the plasma core (ion-root conditions) during the high-density pellet fueled phase of the program. During beginning and ending phases of this program, where the plasma density is lower and $T_e \gg T_i$, a positive core radial electric field is observed. However, in the high density phase of the program where temperature equilibration is achieved a negative radial electric field is developed.

The E_r proflies for selected times in the discharge are shown in Fig.3 along with the

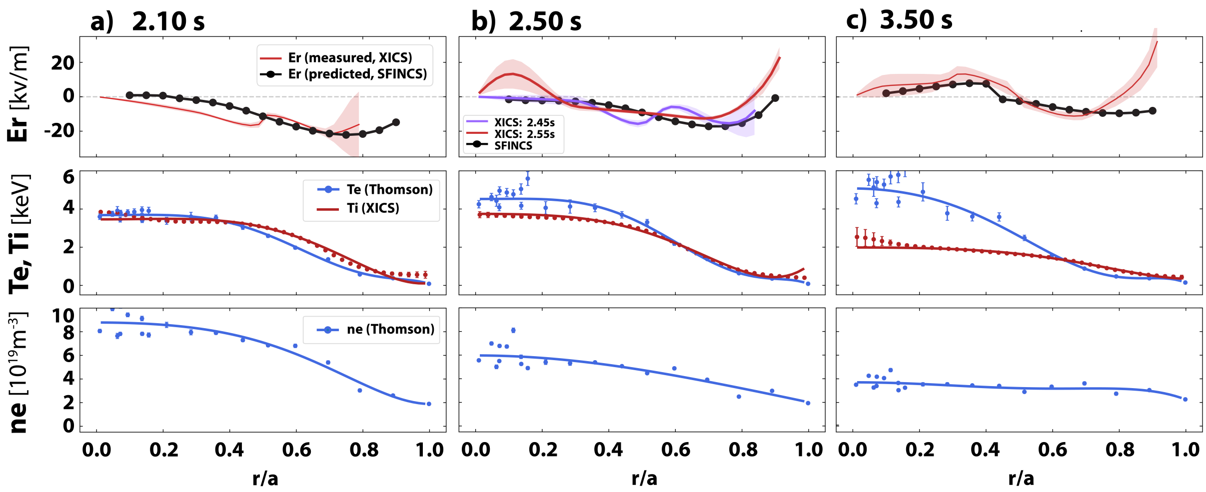

FIG. 3: Comparison of the neoclassical ambipolar radial electric field, calculated using the SFINCS code, with the measured profiles from the XICS diagnostic. Three times are shown which highlight different plasmas conditions found within this discharge. 2.10 s*: Time of peak stored energy, when the plasma is fully within the electron root.* 2.50 s*: Time of transition when the electron root first reappears in the plasma core (E_r profiles from XICS are shown for two consecutive timesilces showing the appearance of the electron root).* 3.50 s*: Steady state period far from the pellet injection where the plasma is in the electron root out to $\rho \approx 0.5$. The shaded region around the measured E_r profiles and the error bars around the temperature and density points correspond to the one sigma error due to photon statistics and are found using a Monte-Carlo procedure. Systematic errors are not shown and may be significantly larger.*

temperature and density profiles. It is important to note that the kinks seen in the E_r profiles are likely due to over-fitting (under-smoothing) during the E_r inversion and not due to the actual profile shape.

The ion-root phase of this program, in which the radial electric field is negative all the way into the plasma core, exists between 1.40 s and 2.50 s, as seen in Fig.2 and highlighted in Fig.1. The precise timing of the ion-root phase has been determined using an analysis completed using a 20 ms integration time (not shown in the current paper), and is expected to be accurate to within this resolution. At the point in which the full ion-root condition develops, at 1.40 s, the following plasmas parameters are observed: $T_{e0} = 2.25\,\mathrm{keV}$, $T_{i0} = 1.75\,\mathrm{keV}$, $\bar{n}_e = 0.45 \times 10^{20}\,\mathrm{m}^{-3}$ and $P_{ECRH} = 2.7\,\mathrm{MW}$. At the start of the transition out of the ion root, at 2.50 s, the following plasma parameters are observed: $T_{e0} = 4.25\,\mathrm{keV}$, $T_{i0} = 3.75\,\mathrm{keV}$, $\bar{n}_e = 0.45 \times 10^{20}\,\mathrm{m}^{-3}$ and $P_{ECRH} = 5.0\,\mathrm{MW}$. Central electron densities at the transition are approximately $0.6 \times 10^{20}\,\mathrm{m}^{-3}$ indicating moderate peaking of the density profile (see Fig.3b). Measurements of the electron temperature and density profiles are taken from the Thomson scattering diagnostic[14] while line integrated measurements of the electron density from the interferometer[15]. At both ends of the ion-root phase we find a similar value of the electron density as well as a similar difference between the absolute ion and electron temperatures, approx 0.5 keV.

Leading up to full development of the ion-root plasma at 1.40 s, it can be observed that an ion root region develops in the outer portion of the plasmas and expands inward. This change in E_r occurs over a time period of around 0.5 s, and can be seen to follow the evolution of the central temperature and density values. Similar behavior is seen as the plasma transitions out of the ion-root after 2.50 s and develops an expanding region of positive radial electric field in the core. The evolution of the E_r inversion radius is highlighted in Fig.2 with dashed lines. The detailed time dependence of changes to E_r profile can be more clearly observed by looking directly at the line-integrated plasma flow measurements shown in Fig.1d. Within the resolution of the available measurements, the electron temperature and velocity appear to change simultaneously, which is consistent with the neoclassical understanding of E_r. These observations of changes in the radial electric field profile in response to changing plasma conditions are in line with studies of the radial electric field at different input powers seen on W7-X[7] and LHD[9].

Leading up to full development of the ion-root plasma at 1.40 s, it can be observed that an ion root region develops in the outer portion of the plasmas and expands inward. This change in E_r occurs over a time period of around 0.5 s, and can be seen to generally follow the evolution of the central temperature and density values. Similar behavior is seen as the plasma transitions out of the ion-root after 2.50 s and develops an expanding region of positive radial electric field in the core. The detailed time dependence of changes to E_r profile can be more clearly observed by looking directly at the line-integrated plasma flow measurements. Within the resolution of the available measurements, the electron temperature and velocity appear to change simultaneously, which is consistent with the neoclassical understanding of E_r. These observations of changes in the radial electric field profile in response to changing plasma conditions are in line with studies of the radial electric field at different input powers seen on W7-X[7] and LHD[9].

4 Neoclassical comparison

The neoclassical (NC) ambipolar radial electric field profile can be found by solving the drift-kinetic equations given a set of temperature and density profiles and a plasma equilibrium. The results of such a calculation, using the SFINCS[16] code, is shown in Fig.3. The profiles used as inputs to the SFINCS calculations are also shown in this figure; the electron temperature and density profiles are taken from the Thomson scattering diagnostic[14], and the ion temperature is taken from the XICS diagnostic. Here the electron density profile has been scaled to match the line-integrated measurements from the interferometer[15] resulting in a scaling factor of 1.1 that has been applied for all times. It is important to note that these NC calculations were done with an approximation of $Z_{eff} = 1$ and a vacuum equilibrium. These approximations have been examined for other W7-X plasmas and are expected to have only a minor effect on the neoclassical results.

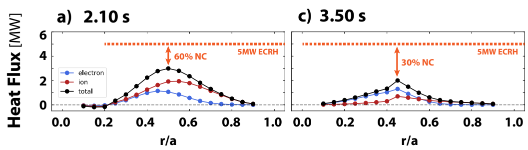

FIG. 4: Neoclassical heat-flux (calculated by SFINCS) as compared to the total input power from ECRH. These calcluations represent the total NC heatflux through a given flux surface.

These neoclassical calculations have been compared to the measured values of E_r and show generally good agreement in both the profile shape and in the magnitude of the results (also seen in Fig.3). This agreement is seen throughout the discharge, and in particular both during the ion-root phase and the electron-root phase. The favorable comparison between calculated and measured E_r provides confidence of the validity of neoclassical calculations and the assumption of ambipolar turbulence for W7-X plasmas.

With this in mind an initial investigation into the role of neoclassical transport in high-density ion-root plasmas is shown in Fig.4. Here the Neoclassical ion and electron heat-flux profiles (Q_{NCi}, Q_{NCe}) are shown for two different times in the plasmas and compared to the total heating power from ECRH. In both the ion-root phase and electron-root phase the electron heat-flux is fairly similar, however the ion heat-flux can be seen to be much more significant during the ion-root phase. This change is significant enough that ions become the dominant NC loss channel during this time.

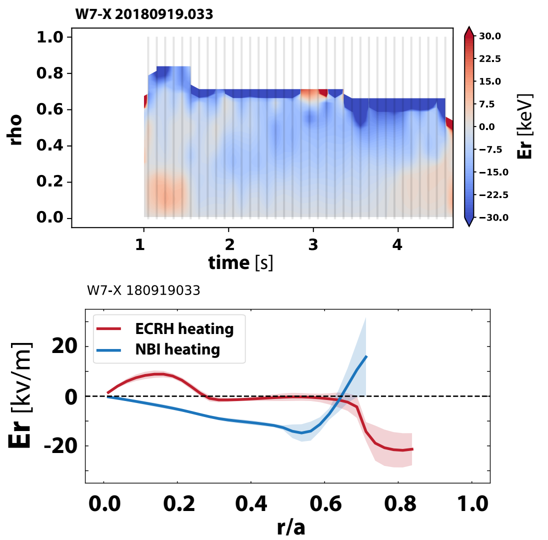

FIG. 5: Measured radial electric field evolution for an NBI heated discharge from the XICS diagnostic. Heating is switched from ECRH to NBI at 1.5 s*. Bottom figure: Profiles of the radial electric field from time just before and after the switch to NBI heating¿*

From the simple comparison between input power and total NC heat flux it can be seen that during the ion-root phase of this discharge approximately 60% of the core transport can be attributed to neoclassical heat-flux, while in the electron-root phase at the end of the discharge less than 30% of core transport can be attributed to NC. In this simple comparison the evolution of the profiles has not been considered; this will not affect the qualitative results but will likely affect the specific percentage given during the ion-root phase. As expected in the outer portion of the plasma NC transport plays a minor role and energy loss is dominated by other sources as turbulent transport, radiation or charge exchange losses.

5 Ion-root in NBI heated plasmas

In addition to ECRH heating, W7-X also has 3.5 MW of neutral beam injection (NBI) heating available. NBI provides not only ion and electron heating, but also a source of core fueling. In plasmas sustained only with neutral beam heating a clear ion-root signature is also observed. The evolution of the measured E_r profiles in a NBI heated discharge (20180919.033) is shown in Fig.5. In beginning of this discharge 2 MW of central ECRH heating is used to provide a background plasma into which NBI can be used. At 1.5 s the ECRH heating is turned off, and heating is switched to 3.5 MW of NBI. The ECRH phase is a typical moderate density W7-X plasma ($n_e = 0.6 \times 10^{20}\,\mathrm{m}^{-3}$, $T_e > T_i$) with a core region of positive radial electric field (electron-root). Immediately after the switch to NBI heating (within 100ms) the radial electric field is found to be negative across the plasmas radius (ion-root). During the NBI phase the density becomes peaked, and T_i is found to be slightly larger than T_e.

6 discussion

Measurements of the core radial electric field (E_r) have confirmed that ion-root conditions (negative E_r in the plasma core) have been achieved in W7-X with high-density plasmas and central ERCH heating. These measured Er profiles agree well with the neoclassical ambipolar Er predicted by the code SFINCS[16]. This good agreement provides confidence in the validity of neoclassical calculations in high-density ion-root conditions, and enables initial studies on the role of neoclassical transport in the optimized high-density regime of W7-X.

Research supported by the U.S. DOE under Contract No. DE-AC02-09CH11466 with Princeton University. This work has been carried out within the framework of the EUROfusion Consortium and has received funding from the Euratom research and training programme 2014-2018 under grant agreement No 633053. The views and opinions expressed herein do not necessarily reflect those of the European Commission.

References

[1] *NÜHRENBERG, J. et al., Physics Letters A* **114** *(1986) 129 .*
[2] *BEIDLER, C. et al., Fusion Technology* **17** *(1990) 148.*
[3] *MAASSBERG, H. et al., Physics of Fluids B: Plasma Physics* **5** *(1993) 3728.*
[4] *WARMER, F. et al., Plasma Physics and Controlled Fusion* **58** *(2016) 074006.*
[5] *MAASSBERG, H. et al., Physics of Plasmas* **16** *(2009).*
[6] *DINKLAGE, A. et al., 43rd EPS Conference on Plasma Physics (2016) O2.107.*
[7] *PABLANT, N. A. et al., Physics of Plasmas* **25** *(2018) 022508.*
[8] *BITTER, M. et al., Review of Scientific Instruments* **81** *(2010) 10E328.*
[9] *PABLANT, N. A. et al., Plasma Physics and Controlled Fusion* **58** *(2016) 045004.*
[10] *PABLANT, N. A. et al., Review of Scientific Instruments* **85** *(2014) 11E424.*
[11] *PABLANT, N. et al., Europhysics Conference Abstracts* **38F** *(2014) P1.076.*
[12] *LANGENBERG, A. et al., 41st EPS Conference on Plasma Physics (2014).*
[13] *PEDERSEN, T. S. et al., Plasma Physics and Controlled Fusion (2018), accepted for publication.*
[14] *PASCH, E. et al., 43rd EPS Conference on Plasma Physics (2016) P4.016.*
[15] *KRYCHOWIAK, M. et al., Review of Scientific Instruments* **87** *(2016) 11D304.*
[16] *LANDREMAN, M. et al., Physics of Plasmas* **21** *(2014).*